Dielectric and Dynamic Mechanical Studies on Homogeneous PBA/PBMA Interpenetrating Polymer Networks

Polycarpos Pissis[1*], Apostolos Kyritsis[1], José Maria Meseguer Dueñas[2], Manuel Monleón Pradas[3], Débora Torres Escuriola[3], Gloria Gallego Ferrer[3] and José Luis Gómez Ribelles[3]

(1) Dept. of Physics, National Technical University of Athens, Zografou Campus, 157 80 Athens, Greece

(2, 3) Center for Biomaterials, Universidad Politécnica de Valencia.

Dept. of Applied Physics (2) and Dept. of Applied Thermodynamics (3),

Camino de Vera s/n, E- 46071 Valencia, Spain

SUMMARY: Broadband dielectric relaxation spectroscopy (DRS, 10^{-2}- 10^{9} Hz), thermally stimulated depolarization currents (TSDC) techniques and dynamic mechanical analysis (DMA) were employed to investigate the dynamic glass transition and, thus, phase morphology in sequential IPNs of poly(butyl acrylate) (PBA) and poly(butyl methacrylate) (PBMA) with 10 weight % of ethyleneglycol dimethacrylate (EGDMA) as branching agent. In a parallel investigation, similar IPNs with only 0.1 % branching agent showed clearly phase separation. In the highly branched IPNs, forced compatibilization induces miscibility of the two components. The results are discussed in terms of suppression of cooperativity and dynamic heterogeneity in the IPNs.

Introduction

An interpenetrating polymer network (IPN) is usually defined as a combination of two or more polymers in network form, at least one of which is synthesized or crosslinked in the immediate presence of the other.[1,2)] A sequential IPN is formed by swelling a polymer network of a first component in the monomer of a second component and then polymerizing the second network. For the majority of IPNs, microphase separation is a characteristic.[1-4)] In polymer blends, polymer miscibility is determined by the composition dependence of the free energy of the blend, subject to thermodynamic equilibrium and stability criteria.[5,6)] In IPNs, the degree of phase mixing may increase due to network formation of chemical or physical bonds between the IPN components.[3,7)] Moreover, in sequential IPNs forced compatibilization of the immiscible IPN components may be achieved if the junction-point density of the component polymerized first is high.[8,9)]

 CCC 1022-1360/00/$ 17.50+.50/0

A widely accepted criterion of miscibility in a two-component polymer system is the occurrence of a single glass transition at an intermediate temperature between the T_g's of the components.[10] However, typically broad glass transitions are measured by differential scanning calorimetry (DSC) in miscible polymer systems.[10] This broadening is, in general, discussed in terms of a distribution of T_g's due to composition fluctuations in the material over dimensions of the order of nanometers, giving rise to nanoheterogeneities.[6,11] The cooperativity length (the size of cooperatively rearranging regions in the Adam-Gibbs theory) is also of the order of a few nanometers at T_g, whereas it decreases significantly with increasing temperature.[12] Thus, the use of dynamic spectroscopic techniques, such as dielectric and dynamic mechanical ones, to investigate the characteristics of the glass transition in miscible polymer systems offers additional possibilities for morphological studies.[6,7] By these techniques the glass transition is probed at temperatures higher than the calorimetric T_g (dynamic glass transition), depending on the frequency of measurement.

In a series of recent papers Donth and coworkers investigated in detail, by a variety of experimental, mostly dynamic, techniques, the splitting of primary, α, and secondary, β, relaxations in the region of the glass transition in poly(n-alkyl methacrylate) homopolymers.[13,14 and references therein] Early work on that point has been summarized in ref.[15] The effects of blending with a second component on that splitting and on the secondary β relaxation have been less systematically studied. The β relaxation appears at lower temperatures and with a lower apparent activation energy in miscible blends of poly(methyl methacrylate), PMMA, and bisphenol-A polycarbonate.[16] In IPNs of PMMA and polyurethane, it is clearly shifted towards lower temperatures with respect to pure PMMA.[3] On the other hand, in miscible blends of PMMA and amorphous poly(vinylidene fluoride), PVDF, the β relaxation appears at the same position as in pure PMMA, whereas the temperature onset of α to β crossover decreases with increasing PVDF content.[17] Finally, dielectric and heat capacity spectroscopy measurements in a series of random copolymers of n-butyl methacrylate with styrene showed that the crossover region simply shifts to a higher frequency with increasing styrene content.[18]

In this work, broad-band dielectric relaxation spectroscopy (DRS), thermally stimulated depolarization currents (TSDC) techniques and dynamic mechanical analysis (DMA) are employed to study phase morphology in sequential IPNs of poly(butyl acrylate) (PBA) and poly(butyl methacrylate) (PBMA), both networks prepared with high junction-point density to

achieve forced compatibilization. A second series of similar IPNs with low junction-point density were prepared and investigated in parallel. The results, to be reported elsewhere, show clearly that, as should be expected, the IPNs of the second series are microphase- separated systems. Our main interest here is focused on studying the effects of forced compatibilization on phase morphology through the investigation of the dynamic glass transition by two dielectric and one dynamic mechanical technique. The results obtained by the various techniques are critically compared with each other.

Experimental Part

Sequential IPNs were prepared by block polymerization using ethyleneglycol dimethacrylate (EGDMA) as branching agent and benzoin (concentration 0.13 wt.-% of monomer) as photoinitiator. The same amount of EGDMA, 10 weight %, was added in the polymerization of both networks of the IPN. PBA was polymerized first. The sheet obtained (of thickness 0.5 to 1.2 mm) was immersed in a solution of BMA monomer and ethanol containing EGDMA and the photoinitiator. Ethanol (up to 40 wt.-%) was used to limit swelling of PBA network in BMA. The swollen sample was exposed to UV light (two UV lamps facing each side of the mold) to polymerize the PBMA network. The Philips 8W lamps yielded 90% of radiation between 300 and 420 nm, maximum being at 365 nm. Low mass substances were extracted from the IPN by boiling in ethanol for 24 h and then drying in vacuum to constant weight. The IPNs are designated as IPNXX, where XX indicates the weight % of PBA network in the IPN. XX was varied between 32 and 81 weight % by varying the ratio of BMA/ ethanol in the second polymerization step. The pure PBMA network crosslinked with 10 weight % EGDMA was also prepared following the same routine as in the case of the PBA network. In the second series of PBA/ PBMA IPNs studied in a parallel investigation (the microphase-separarted systems) the junction-point density was only 0.1 %.

For broad-band DRS measurements between 10^{-2} and 10^{9} Hz the sample was sandwitched between nickel-coated stainless steel or gold-coated brass electrodes. Details of the equipment used have been given elsewhere.[19] The TSDC method consists of measuring the thermally activated release of stored dielectric polarization and corresponds to measuring dielectric losses against temperature at low frequencies of 10^{-2} - 10^{-4} Hz.[20] The equipment and the procedure used for TSDC measurements in the temperature range from –185 to 30 °C have

been described elsewhere.[7,21)] For DMA measurements a Seiko DMS210 instrument was used at frequencies 0.1, 1 and 10 Hz.

Results and Discussion

Fig. 1 and 2 show isochronal (constant frequency) temperature plots of the mechanical loss tangent, tanδ, in DMA experiments at 1 Hz and of the dielectric losses, ε'', in DRS experiments at 1 kHz, respectively, for all the compositions studied. For comparison, Fig. 3 shows the TSDC thermograms for the PBA- rich samples. The equivalent frequency of TSDC measurements is in the range 10^{-2}- 10^{-4} Hz.[20, 21)]

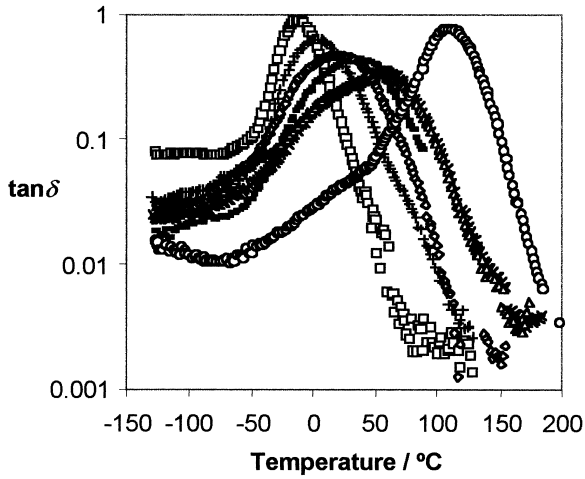

Fig. 1: Loss tangent tanδ vs. temperature measured by DMA at 1 Hz in PBA(□), IPN81 (+), IPN67 (◇), IPN56 (–), IPN45 (△), IPN36 (×) and PBMA (○).

The tanδ peak in Fig. 1 for the pure PBA network corresponds to the primary, α relaxation associated with the glass transition. In the corresponding peak for the pure PBMA network, a shoulder is observed on the low- temperature side, attributed to the secondary, β relaxation of Goldstein- Johari type.[13, 14)] In the IPNs, a broad tanδ peak is observed located between those in the pure networks and shifting to lower temperatures with increasing PBA content. This is interpreted in terms of a homogeneous morphology. We will come to this point later. The peak becomes broader in the PBMA-rich samples, probably because of the contribution of the PBMA β relaxation. However, it cannot be fully excluded at this stage that two α relaxations with composition-dependent peak temperatures, corresponding to the glass transitions of

PBA- and PBMA-rich microphases, contribute to the broad tanδ peaks. In the plot of the elastic modulus, E', versus temperature, the counterpart of the plot in Fig. 1, not shown here, it can be seen that E' in the rubbery state is higher in some IPNs than in any of the pure networks. It follows that the average molar mass $<M>$ between junction-points, calculated according to the theory of rubber elasticity ($<M>$ = 2300 g·mol^{-1} in PBA), is in these IPNs smaller than in the pure networks. This feature has to be explained by the appearance of mutual entanglements between the two networks acting as new junctions in the IPNs and provides additional support for miscibility of the two networks.

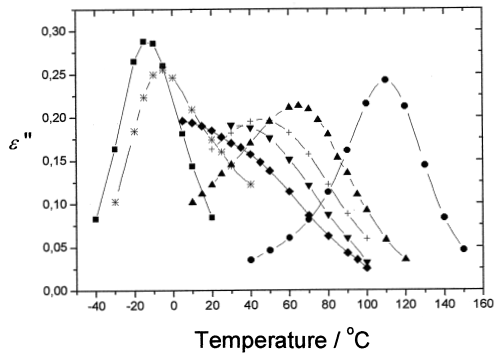

Fig. 2: Dielectric loss ε'' vs. temperature measured by DRS at 1 kHz in PBA(■), IPN81 (✳), IPN67 (◆), IPN56 (▼), IPN45 (+), IPN36 (▲) and PBMA (●).

Most of the comments to Fig. 1 are also relevant to the dielectric results in Fig. 2. The differences between the two figures are due to the different sensitivities of dielectric and mechanical techniques to molecular motions (different relative intensities and temperature-frequency positions of the α and β relaxations[13-15]) and to the different frequencies used (1 Hz in DMA against 1 kHz in DRS). The TSDC plot in Fig. 3 shows the α relaxation at high temperatures, shifting to higher temperatures with decreasing PBA content, similar to the results shown in Fig. 1 and 2, but limited only to three compositions, because of the limited temperature range of TSDC measurements in this work. The characteristic temperatures of the α relaxation obtained by the various techniques will be quantitatively compared with each other later. The TSDC plots in Fig. 3 show a weak peak at about –120 °C. This peak, observed also in DMA experiments at about –85 °C at 1 Hz, corresponds to the local β relaxation in PBA.[15] In contrast to the TSDC α peak, the TSDC β peak does not shift with composition, in agreement with the observation that local relaxations are less affected by blending.[7]

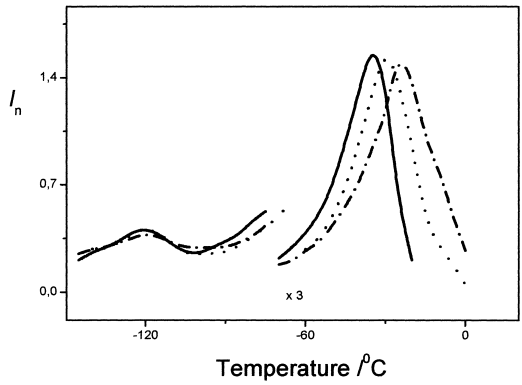

Fig. 3: TSDC thermograms obtained with PBA (—), IPN81 (· · · ·) and IPN67 (– · – ·).

The DMA and TSDC data in Fig. 1 and 3, respectively, have been recorded directly in the temperature domain (isochronal temperature scans). The DRS data were recorded in the frequency domain (isothermal frequency scans) and replotted to give Fig. 2. An example of isothermally recorded DRS data is given in Fig. 4, which shows $\varepsilon''(f)$ for IPN36 at several temperatures. A broad peak is observed that, with increasing temperature of measurement, shifts to higher frequencies, increases in magnitude and becomes significantly more narrow. Similar measurements, typically extended to 10^9 Hz (not shown in Fig. 4), were performed with all the compositions. The data have been treated using well established procedures[4,7,13] to obtain information from the frequency position, the magnitude and the shape of the loss peaks and their changes with temperature. The most significant results will now be presented.

Fig. 5 shows the Arrhenius plot for the dielectric data for all the compositions. The loss peaks, similar to those shown in Fig. 4, have been considered as single peaks, f_{max} in Fig. 5, being the frequency of maximum loss. For the compositions IPN56 and IPN67, two loss peaks have been observed in the temperature and frequency ranges of the measurements, so at many temperatures two values of f_{max} are given in Fig. 5 for these compositions. The data for pure PBA and the compositions PBA81 and PBA67 (high frequency peak for that composition) show the typical behaviour of a dynamic glass transition. The Vogel-Tammann-Fulcher-Hesse (VTFH) equation.[12,19]

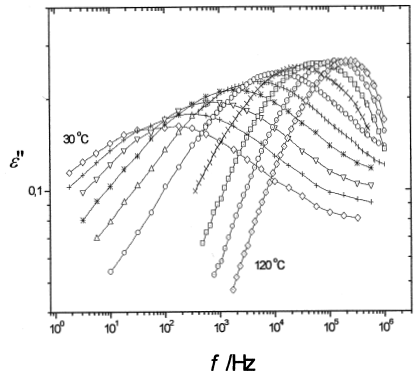

Fig. 4: Dielectric loss ε'' vs. frequency f in IPN36 at several temperatures between 30 (-◇-) and 120 °C (-◈-) in steps of 10 °C.

$$f_{\max} = A\exp\left(-\frac{B}{T-T_o}\right) \tag{1}$$

where A, B and T_o (Vogel temperature) are temperature independent empirical parameters, was fitted to the data for these three samples and reasonable values of the fitting parameters were obtained. An example of a fitting is shown in Fig. 5 for the pure PBA network, for which the fitting parameters take the values A= 1.4×10^{13} Hz, B= 1969 K and T_o= 174.5 K.

For the pure PBMA network, the raw dielectric data ($\varepsilon''(f)$ at several temperatures, not shown here) suggest, in agreement with data in the literature[13,15], a splitting of the single $\alpha\beta$ (or a) relaxation at high temperatures (or lower frequencies) into two relaxations, α and β, at lower temperatures. One, or a sum of two Havriliak-Negami (HN) functions[22] of the type

$$\varepsilon^*(\omega) = \varepsilon_\infty + \frac{\Lambda\varepsilon}{\left[1+\left(\frac{i\omega}{\omega_o}\right)^{1-\alpha}\right]^\gamma} \tag{2}$$

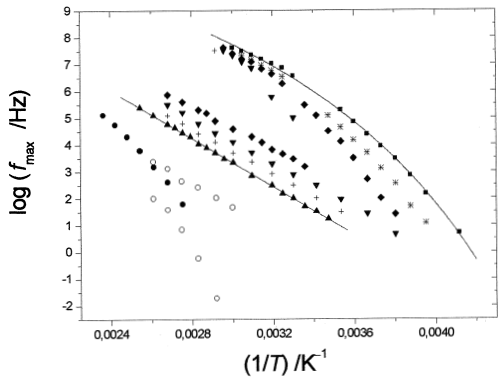

Fig. 5: Arrhenius plot of the DRS data in PBA(■), IPN81 (✱), IPN67 (◆), IPN56 (▼), IPN45 (+), IPN36 (▲) and PBMA (raw data ●, and data obtained by analysis ○, details in text). The lines are fittings of Eq. (1) to the PBA data and Eq. (3) to the IPN36 data. Note that two relaxations are observed for the compositions IPN56 and IPN67, see the text for details.

and an additional conductivity term ($\sim\omega^{-s}$, $s \leq 1$) were fitted to the ε''(f) data for the PBMA network. In equation (2) $\varepsilon^* = \varepsilon' - i\varepsilon''$, $\omega = 2\pi f$, ω_0 is the position on the angular frequency scale of the relaxation process, ε_∞ is $\varepsilon'(\omega)$ for $\omega >> \omega_0$, $\Delta\varepsilon$ is the relaxation strength and α and γ the shape parameters. The results of this analysis are also shown in Fig. 5. For $T \leq 110$ °C a sum of two HN functions gave better fits than one. In linear PnBMA with $T_g = 24$ °C, lower than in the PBMA network under investigation, this change from one to two HN functions occurred at 80 °C.[13] The shape parameters $(1-\alpha)$ and $(1-\alpha)\gamma$ give the slope of $\varepsilon''(f)$ at frequencies lower and higher, respectively, than the peak frequency.[19] They take the value 1 for a Debye peak. With the temperature decreasing from 110 to 70 °C, for the α peak $(1-\alpha)$ decreases from 0.64 to 0.56 and $(1-\alpha)\gamma$ from 0.35 to 0.23. For the β peak $(1-\alpha)$ decreases from 0.48 to 0.42 and $(1-\alpha)\gamma$ from 0.34 to 0.26 in the same range of temperatures. It follows that both peaks are asymmetric (steeper at lower frequencies) and become broader with decreasing temperature and that, at each temperature, the β peak is broader than the α peak.[13] Following the analysis proposed by Donth and coworkers,[13] the onset temperature of the α relaxation can be determined from a plot of the temperature dependence of the relaxation strength $\Delta\varepsilon$ to about 120 °C (against 110 °C for linear PnBMA).[13]

The dielectric data in Fig. 5 for the compositions IPN36, IPN45, IPN56 and IPN 67 (the low-frequency relaxation for the last two compositions) suggest a linear dependence, with a slope similar to that for the β relaxation in the pure PBMA network. As an example, a fit of the Arrhenius equation

$$f_{\max} = f_o \exp\left(-\frac{W}{kT}\right) \tag{3}$$

where f_o a constant, W the activation energy and k Boltzmann's constant, to the IPN36 data has been included in Fig. 5. The fitting parameters are W= 0.90 eV and f_o= 7.4×10^{16} Hz. These results suggest a suppression of cooperativity (giving rise to the VTFH behavior) in the IPNs that may be discussed in terms of constraints imposed by junction-points, entanglements, and confinement.[23] On the other hand, with increasing PBA content, $f_{\max}$ shifts, at constant frequency, to lower temperatures towards the result for PBA, like the α relaxation should do. In addition, the values of W and f_o are rather high for one- barrier activation, as commonly assumed for local relaxations. Donth and coworkers interpreted high values of W and f_o for the β relaxation in poly(n-alkyl methacrylate)s as indicative of the coordinated motion of neighbouring side chains and introduced[13] the term "locally coordinative".

For the compositions IPN56 and IPN67, two relaxations are observed by DRS (Fig. 5), one of them with characteristics similar to those of the α relaxation in PBA and the other corresponding to the mean composition. These results may be discussed in terms of dynamic heterogeneity[24] and a model proposed by Kumar et al.[6]

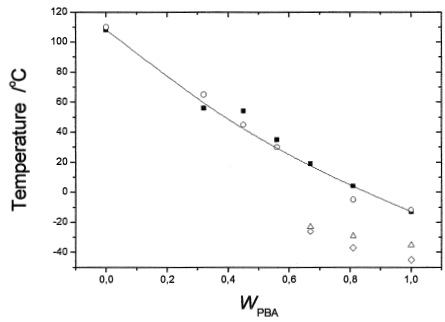

Fig. 6: Temperature of DMA tanδ peak at 1 Hz (■), temperature of DRS loss peak at 1 kHz (○), temperature of TSDC peak (△) and $T_{g\ \mathrm{diel}}$ (◇) vs. composition of the IPNs. The curve represents the Fox equation, details in text.

Fig. 6 compares characteristic temperatures of the dynamic processes in the IPNs: the temperature of the DMA tanδ peak at 1 Hz (Fig. 1) and the temperature of the DRS loss peak at 1 kHz (Fig. 2) (the low frequency peak for the compositions IPN56 and IPN67). For the PBA rich samples two more temperatures have been included: that of the TSDC α peak (Fig. 3) and $T_{g\,diel}$, defined by the condition $f_{max}(T_{g\,diel})= 1.6\times10^{-3}$ Hz[19] and obtained by extrapolation of the data in Fig. 5 to low frequencies. All the characteristic temperatures show the same trend of increasing with decreasing PBA content. For a detailed discussion, the time scale, defined by the frequency of measurement, and the spatial scale, given by the type of motion probed, should be considered. In addition, it should be taken into account that a modulus is measured by DMA, whereas a compliance is measured by DRS, and that the characteristic temperatures refer to tanδ for DMA and to ε'' for DRS.[25] The curve in Fig. 6 is given by the Fox equation[26] for a homogeneous mixture,

$$\frac{1}{T} = \frac{w_{PBA}}{T_{PBA}} + \frac{(1 - w_{PBA})}{T_{PBMA}} \tag{4}$$

where T_{PBA} and T_{PBMA} the characteristic DMA temperatures of the pure networks (Fig. 1), which coincide with the DRS (1 kHz) temperatures. It describes well the DMA and the DRS (1 kHz) data, providing additional support for miscibility achieved by forced compatibilization.

Conclusions

The main results of this work are summarized in Figs. 5 and 6. They suggest that forced compatibilization induces miscibility of the PBA and PBMA components, suppression of cooperativity in the PBMA-rich compositions and dynamic heterogeneity in the intermediate compositions. It would be interesting to extend the analysis to other parameters of the dynamic glass transition, such as the multiplicity of relaxation times and the fragility (for the PBA- rich compositions). Work along these lines is in progress, as well as measurements in analogous systems, poly(ethyl acrylate)/ poly (ethyl methacrylate) sequential IPNs.

Acknowledgement

J.M.M.D. acknowledges the support of the Generalitat Valenciana through project CV97-TI-06-36

References

1. L. Sperling, *Interpenetrating Polymer Networks and Related Materials*, Plenum Press, New York 1981
2. D. Klempner, K.C. Frisch (Eds.), *Advances in Interpenetrating Polymer Networks*, Volume IV, Technomic Publishing, Lancaster (PA) 1994
3. A.K. Rizos, G. Fytas, R.J. Ma, C.H. Wang, V. Abetz, G.C. Meyer, *Macromolecules* **26**, 1869 (1993)
4. A. Kanapitsas, P. Pissis, L. Karabanova, L. Sergeeva, L. Apekis, *Polym. Gels Networks* **6**, 83 (1998)
5. C.M. Roland, K.L. Ngai, *Macromolecules* **25**, 363 (1992)
6. S.K. Kumar, R.H. Colby, S.H. Anastasiadis, G. Fytas, *J. Chem. Phys.* **105**, 3777 (1996)
7. G. Georgoussis, A. Kyritsis, V.A. Bershtein, A.M. Fainleib, P. Pissis, *J. Polym. Sci. Part B Polym. Phys.*, in press
8. B.Y. Li, X.P. Bi, D.H. Zhang, F.S. Wang, in: *Advances in Interpenetrating Polymer Networks*, Volume I, D. Klempner, K.C. Frisch (Eds.), Technomic Publishing, Lancaster (PA) 1989
9. D.G. Fradkin, J.N. Foster, L.H. Sperling, D.A. Thomas, *Polym. Engn. Sci.* **26**, 730 (1996)
10. J.M.G. Cowie, S. Harris, J.L. Gomez Ribelles, J.M. Meseguer, F. Romero, C. Torregrosa, *Macromolecules* **32**, 4430 (1999)
11. M. Bank, J. Leffingwell, C. Thies, *Macromolecules* **4**, 1971 (1971)
12. E. Donth, *Relaxation and Thermodynamics in Polymers. Glass Transition*, Akademie Verlag, Berlin 1992
13. F. Garwe, A. Schoenhals, H. Lockwenz, M. Beiner, K. Schroeter, E. Donth, *Macromolecules* **29**, 247 (1996)
14. M. Beiner, K. Schroeter, E. Hempel, S. Reissig, E. Donth, *Macromolecules* **32**, 6278 (1999)
15. N.G. McCrum, B.E. Read, G. Williams, *Anelastic and Dielectric Effects in Polymeric Solids*, Wiley, London 1967
16. J.T.C. Landry, P. Mark Heinrichs, *Macromolecules* **22**, 2157 (1989)
17. J. Wing Sy and J. Mijovic, *Macromolecules* **33**, 933 (2000)
18. S. Kahle, J. Korus, E. Hempel, R. Unger, S. Hoering, K. Schroeter, E. Donth, *Macromolecules* **30**, 7214 (1997)
19. A. Kyritsis, P. Pissis, S.-M. Mai, C. Booth, *Macromolecules* **33**, 4581 (2000)
20. J. van Turnhout, in: *Electrets, Topics in Applied Physics*, Volume 33, G.M. Sessler (Ed.), Springer Verlag, Berlin 1980
21. P. Pissis, A. Anagnostopoulou- Konsta, L. Apekis, D. Daoukaki-Diamanti, C. Christodoulides, *J. Non-Cryst. Solids* **131- 133**, 1147 (1991)
22. S. Havriliak, S. Negami, *J. Polym. Sci., Polym. Symp.* **14**, 89 (1966)
23. V.A. Bershtein, L.M. Egorova, P.N. Yakushev, G. Georgoussis, A. Kyritsis, P. Pissis, P.S. Sysel and L. Brozova, *Macromol. Symp.* **146**, 9 (1999)
24. J.B. Miller, K.J. McGrath, C.M. Roland, C.A. Trask, A.N. Garroway, *Macromolecules* **23**, 4543 (1990)
25. A.S. Vatalis, C.G. Delides, O.P. Grigoryeva, L.M. Sergeeva, A.A. Brovko, O.N. Zimich, V.I. Shtompel, G. Georgoussis, P. Pissis, *Polym. Engn. Sci*, in press
26. T.G. Fox, *Bull. Am. Phys. Soc.* **1**, 123 (1956)